View metadata, citation and similar papers at core.ac.uk
brought to you by CORE
provided by Italian Group Fracture (IGF): E-Journals / Gruppo Italiano Frattura

A. Carofalo et alii, Frattura ed Integrità Strutturale, 30 (2014) 349-359; DOI: 10.3221/IGF-ESIS.30.42

Focussed on: Fracture and Structural Integrity related Issues

Modification of creep and low cycle fatigue behaviour induced by welding

A. Carofalo, V. Dattoma, R. Nobile, F.W. Panella
Università del Salento - Dipartimento di Ingegneria dell'Innovazione, Via per Arnesano, 73100 Lecce, Italy
alessio.carofalo@unisalento.it; vito.dattoma@unisalento.it; riccardo.nobile@unisalento.it; francesco.panella@unisalento.it

G. Alfeo
GE Avio srl– Ingegneria – Ricerca e Sviluppo Tecnologico, via Angelo Titi 16, 72100 Brindisi, Italy
Giovanni.Alfeo@avioaero.com

A. Scialpi
GE Avio srl – Ingegneria – Progettazione Componenti Motori, via Arno 60 Angelo Titi 16, 72100 Brindisi, Italy
Agostino.Scialpi@avioaero.com

G.P. Zanon
GE Avio srl – Ingegneria – Ricerca e Sviluppo Tecnologico, via I Maggio 99, 10040 Rivalta di Torino (TO), Italy
Giovanni.Zanon@avioaero.com

ABSTRACT. In this work, the mechanical properties of Waspaloy superalloy have been evaluated in case of welded repaired material and compared to base material. Test program considered flat specimens on base and TIG welded material subjected to static, low-cycle fatigue and creep test at different temperatures.
Results of uniaxial tensile tests showed that the presence of welded material in the gage length specimen does not have a relevant influence on yield strength and UTS. However, elongation at failure of TIG material was reduced with respect to the base material.
Moreover, low-cycle fatigue properties have been determined carrying out tests at different temperature (room temperature RT and 538°C) in both base and TIG welded material. Welded material showed an increase of the data scatter and lower fatigue strength, which was anyway not excessive in comparison with base material. During test, all the hysteresis cycles were recorded in order to evaluate the trend of elastic modulus and hysteresis area against the number of cycles. A clear correlation between hysteresis and fatigue life was found.
Finally, creep test carried out on a limited number of specimens allowed establishing some changes about the creep rate and time to failure of base and welded material. TIG welded specimen showed a lower time to reach a fixed strain or failure when a low stress level is applied. In all cases, creep behaviour of welded material is characterized by the absence of the tertiary creep.

KEYWORDS. Low-cycle fatigue; Welding; Fatigue damage; Nickel-base superalloys.

INTRODUCTION

Design of gas turbine engine components is influenced by repeated request of higher performances in terms of high power, efficiency improvement, reduction of weight and costs. Another important point is the reliability of the design model used, that determines the flight safety. These objectives are generally achieved following two approaches: firstly, the development of material that could increase the maximum working temperature and could have a direct impact on the performance of the gas turbine; secondly, the development of advanced modelling techniques that could lead to the reduction of the safety factors generally used in the design phase.
Thermomechanical damage is the main limiting factor of the life in a Nickel-based superalloy mechanical component [1]. Complex loads often lead to severe non-linear material behaviour, such as creep deformation and fatigue, while high temperature increases the probability of localized material plasticization under the service loads. Therefore, design against fatigue failure utilizes fatigue behaviour obtained through strain control fatigue tests. Creep and fatigue damages are generally studied using different models, even if some attempts to unify the material behaviour can be reached in literature [2, 3]. Anyway, these models were developed and experimentally verified for high strain levels in case of fatigue and for high stress-temperature condition in case of creep. The extension of their prediction to moderate strain levels, where elastic behaviour is predominant, constitutes a serious limitation [4].
Nucleation of fatigue crack represents the critical phenomenon that lead to failure of Nickel-based components [5-7]. From a metallurgical point of view, Nickel-based superalloys at high temperature are characterized by a change of ductility and the formation of an oxidation film on the surface. These two phenomena are antithetical with respect to the fatigue damage: the softening of the metallic matrix causes an increase of the probability of a fatigue crack initiation, while crack nucleation and propagation is interfered by oxide layer on the surface [8]. The combination of these factors determines the behaviour of the considered material. The interaction of creep and fatigue phenomena is a further complication and it is a phenomenon not well understood [9].
In this work, the mechanical properties of base material and TIG welded Waspaloy have been compared carrying out static, low-cycle fatigue and creep test on specimen obtained by a laminated sheet having a nominal thickness of 3.1 mm. In most cases, fatigue tests have been carried out with applied strain range $\Delta\varepsilon \leq 0.6\%$. This kind of low stress level is associated to limited damage process. In this condition, the damage models are generally inapplicable or lead to inconsistent prediction. On the other hand, material behaviour at this stress level is very useful for industrial application, since it is close to component working condition. Therefore, simple and quick indicators of the different behaviour performance for static, fatigue and creep properties have been chosen and calculated, both for base and TIG welded material. The reduction of performances originated by welding has been estimated by the percentage variation of these indicators.

MATERIAL AND EXPERIMENTAL PROCEDURE

Waspaloy is a conventional Nickel-based superalloy that is subjected to hardening precipitating heat-treating. Waspaloy is widely used in the aeronautical field due to its good strength to corrosion and to high temperature, in particular for the realization of turbine disk, blade and casing. Mechanical strength is comparable to Haynes R-41 and higher than Inconel 718 at temperature higher than 650-705°C [8]. Microstructure is characterized by a face centered cube matrix with dominant precipitates γ'. Ductility of Waspaloy has been studied in [10], showing a reduction starting from room temperature to about 300 °C, an irregular behaviour up to 600 °C and a quick reduction at higher temperature.
Waspaloy can be welded using conventional or advanced welding techniques. In presence of a localized damage in a large high-cost component, a possible maintenance strategy is to repair it removing the damage zone and substituting it with welded material. The residual life of the component would be increased with evident economic advantages, on condition that the reliability and the safety of the component are not reduced. Weldability of Waspaloy from a technological and metallurgical point of view has been studied in [11, 12]. Generally speaking, the fusion and the following solidification determine at least grain growth and introduce defect like microcracks. From a macroscopic point of view, these phenomena produce a reduction in ductility, showed by lower elongation at failure and lower fatigue and creep strength [13-17].
Starting from a laminated plate having a nominal thickness of 3.1 mm, base material specimens for static, fatigue and creep tests have been realized. At the same time, a similar plate has been butt-welded using an optimized TIG process in

order to avoid the introduction of microdefects in the weld cord both in the as-welded condition and after PWHT heat-treating. TIG welded specimens are obtained taking care to guarantee the presence of a transversal welding cord in the specimen gage length. Weld cord has been removed through flattening and the welded plate has been subjected to an optimized aging heat-treating. Finally, specimens have been obtained by cutting and milling. However, thermal cycle of welding, aging heat-treating and final milling introduced specimen distortions, which was not compatible with the standard required for the execution of the mechanical tests, in particular low-cycle fatigue tests. Therefore, specimens have been plastically deformed at room temperature to respect the straightness tolerance.

Flat specimens are not the usual choice to carry out high temperature mechanical test, due to the highest difficulty for a correct load application and a reliable strain measurement. However, a particular care has been used in order to achieve correct results from the mechanical test. Since a three-zone split furnace was used for heating, load application to specimen was obtained through serrated face grip designed and realized in Udimet720. This grip allows the application of a preload to the specimen in order to guarantee the backlash recover especially during low-cycle fatigue test. Even if the dimension of the specimen were opportunely reduced to limit the maximum load, grip was subjected to severe creep and plastic deformation that requires its substitution to complete the experimental program.

Static test has been carried out following the indication of ASTM E8-04 and E21-09 standards, respectively for room temperature (RT) and high temperature 503°C, 704°C and 760°C. Sub-size specimen has been used for test at 503°C, in order to limit the maximum load during test. All the tests are carried out in displacement control imposing a speed of 0.1 and 0.5 mm and repeated on 3 and 5 specimens, respectively for room and high temperature. Test temperature is measured and controlled in three point using K thermocouples in contact in three different point of the specimen gage length.

Low-cycle fatigue tests are carried out following the indication of ASTM E606-04 standard, using a triangular waveform in strain control and a frequency of 0.5 Hz. Specimen geometry has been changed with respect to the standard indication increasing the fillet radius to a value of 15 mm, in order to avoid failure due to excessive stress concentration (Fig. 1a). It was verified that this geometry was able to hold compressive strength close to yield strength without showing buckling and transversal deflection of the specimen. All the test are characterized by a strain ratio $R_\varepsilon = \varepsilon_{min}/\varepsilon_{max} = 0$. Applied strain is in the range $\Delta\varepsilon$ = 0.4-0.9 %, therefore plastic deformation is low or absent and the expected fatigue life is relatively high. Run-out level was fixed at 10^5 cycles, after which test is continued in load control using the stabilized cycle stress range. Experimental test plan considers tests at room temperature (RT), 538°C and 760°C, both for base and TIG welded material. In this work only the results of RT and 538°C conditions are showed and discussed.

Static and low-cycle fatigue tests were carried out on a servohydraulic testing machine 100 kN MTS810, while extensometers used for strain control test have a 10 mm gage length.

Creep test are carried out on a dead-weight creep machine NORTEST TC50 equipped with adapters for flat specimen, which geometry is reported in Fig. 1b. Two different stress levels and a temperature of 704°C have been considered. Each test condition has been repeated on three specimens to guarantee the repeatability of the result.

EXPERIMENTAL RESULTS AND DISCUSSION

Static test

Static behaviours of laminated Waspaloy obtained in this work are resumed in Tab. 1, which reports the mean values of the most representative static parameters. All the values have been normalized considering a reference value equal to maximum strength. Yielding stress and tensile strength of the base material are coherent with the data reported in literature for Waspaloy [10, 18]. At temperature above 700°C, hardening disappeared justifying the decay of the tensile strength at high temperature. Finally, Young modulus undergoes a reduction of about 50% at 760°C, which is higher than that reported in literature for Waspaloy. A wide extension of the plastic zone is observed at temperature above 700°C (Fig. 2a), which is in contrast with the marked reduction observed in [10].

Assuming base material as a reference, the modification of the static behaviour induced by TIG is clearly highlighted. If the variability of yielding stress and Young modulus is excluded, which are data sensitive to error and numerical manipulation during elaboration, tensile strength is practically not affected by the presence of weld cord. As expected, a relevant change consists in a reduction of the plastic zone in all the condition. In particular, at the highest temperature, the presence of the weld cord restrained the extension of the plastic zone that was found for the base material (Fig. 2b).

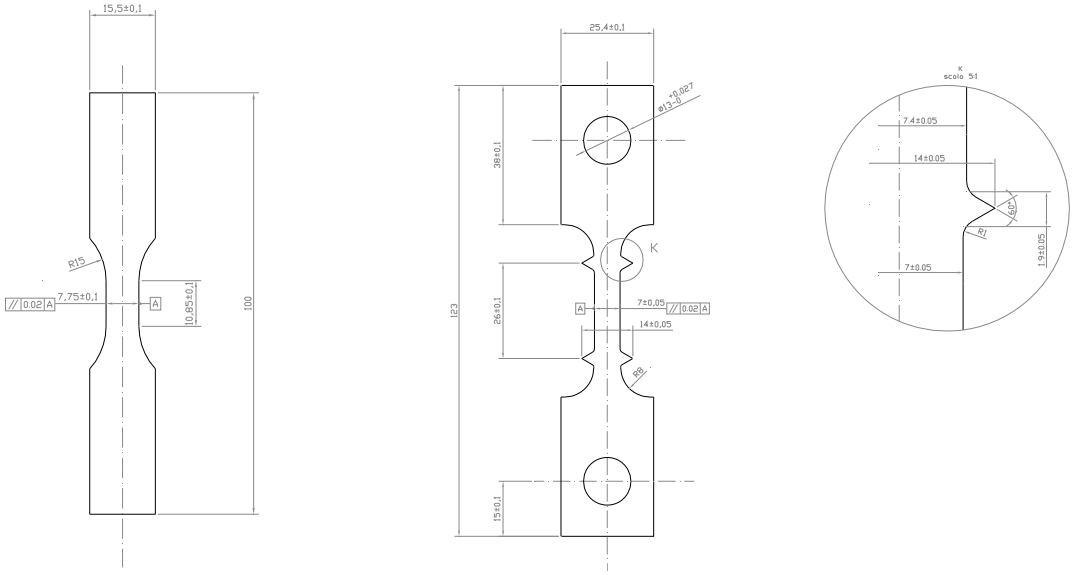

(a) (b)

Figure 1: Specimen geometry for LCF test (a) and creep test (b).

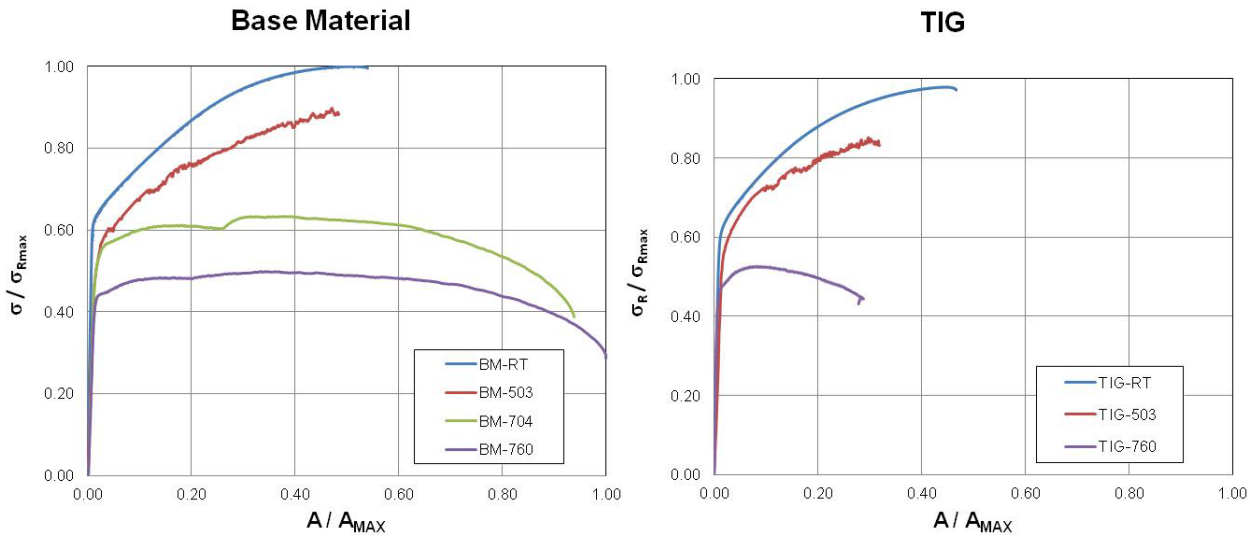

(a) (b)

Figure 2: Static behaviour of base (a) and TIG welded (b) material.

	Yielding Stress σ_y [N/mm²]			*Tensile Strength* σ_R [N/mm²]			*Elongation to Failure* A [%]			*Young Modulus* E [N/mm²]		
	Base Material	*TIG*	*var %*	*Base Material*	*TIG*	*var %*	*Base Material*	*TIG*	*var %*	*Base Material*	*TIG*	*var %*
RT	0.617	0.622	0.78	1	0.968	-3.24	0.65	0.43	-33.64	1	0.948	-5.22
503°C	0.519	0.484	-6.7	0.867	0.836	-3.58	0.47	0.34	-28.18	0.738	0.658	-10.83
704°C	0.516	-	-	0.607	-	-	0.93	-	-	0.571	-	-
760°C	0.444	0.446	0.53	0.497	0.514	3.39	1	0.25	-75.00	0.522	0.560	7.27

Table 1: Static behaviour of base and TIG welded material.

Low-Cycle Fatigue test

Relevant data about the fatigue tests are resumed in Tab. 2-5 for each test condition. All the data are normalized with respect to a reference value corresponding to the maximum one. Failure is identified by a decay of 10 % of the maximum stress with respect to the stabilized cycle. Specimens that reached the run-out level of 10^5 cycles are marked in **bold** to indicate that the test was completed in load control up to failure. In the same tables, several indicators are reported, referred to the stabilized cycle, which is generally identified as the half-life cycle. In particular, the stress range, stress ratio R, tangent elastic modulus E_T and the amount of the hysteresis area H have been calculated and showed.

	Strain Range $\Delta\varepsilon/\Delta\varepsilon_{max}$	*Cycles to failure* N_f/N_{max}	*Normalized Stress Range* $\Delta\sigma/\Delta\sigma_{max}$	*Stress Ratio* $R = \sigma_{min}/\sigma_{max}$	*Hysteresis Area* $H\ [mJ/mm^3]$	*Tangent Modulus* $E_T\ [N/mm^2]$
MB-RT-1	0.984	0.0037	1.0000	-0.86	1.536	214109
MB-RT-2	0.879	0.0045	0.9798	-0.74	0.886	218793
MB-RT-3	0.771	0.0093	0.8824	-0.66	0.329	212641
MB-RT-4	0.686	0.0136	0.8408	-0.64	0.151	224218
MB-RT-5	0.581	0.0310	0.7667	-0.97	0.040	235026
MB-RT-6	0.795	0.0077	0.9620	-0.97	0.549	229147
MB-RT-8	0.790	0.0087	0.9492	-0.84	0.500	226862
MB-RT-9	0.562	0.0223	0.7410	-0.40	0.035	226357
MB-RT-10	0.564	**0.1611**	0.7563	-1.64	0.015	228901
MB-RT-11	0.602	0.0180	0.7832	-0.54	0.051	231935
MB-RT-13	0.461	**0.0621**	0.6062	-0.48	0.009	232259
MB-RT-14	0.460	0.0436	0.5952	-0.28	0.012	230506
MB-RT-15	0.459	**0.0562**	0.6050	-0.61	0.053	231954
MB-RT-16	0.460	0.0432	0.5511	-0.24	0.026	216363

Table 2: Base Material – Room Temperature: fatigue test results.

	Strain Range $\Delta\varepsilon/\Delta\varepsilon_{max}$	*Cycles to failure* N_f/N_{max}	*Normalized Stress Range* $\Delta\sigma/\Delta\sigma_{max}$	*Stress Ratio* $R = \sigma_{min}/\sigma_{max}$	*Hysteresis Area* $H\ [mJ/mm^3]$	*Tangent Modulus* $E_T\ [N/mm^2]$
MB-538-1	0.789	**0.3191**	0.5377	-0.36	0.051	118358
MB-538-3	0.697	**0.4474**	0.4091	-0.11	0.024	106123
MB-538-4	0.785	**0.4518**	0.4354	0.00	0.291	114078
MB-538-5	1.000	0.0040	0.6852	-0.52	0.392	123529
MB-538-6	0.880	0.0102	0.6565	0.56	0.065	129012
MB-538-8	0.890	0.0127	0.6001	-0.37	0.231	131086
MB-538-9	0.950	0.0030	0.7795	-0.80	0.378	154759
MB-538-10	0.786	**0.0526**	0.5511	-0.13	0.405	160511
MB-538-11	0.973	**0.0396**	0.6375	-0.40	0.179	100070
MB-538-12	0.895	**0.1313**	0.5450	-0.40	0.464	132828
MB-538-13	0.898	**0.1002**	0.5622	-0.37	0.190	101577
MB-538-14	0.786	**0.3942**	0.4440	-0.14	0.023	103100
MB-538-16	0.981	0.0034	0.6944	-0.31	0.153	115671

Table 3: Base Material – 538°C: fatigue test results.

The application of load cycle in strain control originates non-linear phenomenon within the material. The applied work can be divided in potential and dissipated energy and several predictive models based on macroscopic energy approaches have been developed to evaluate fatigue damage. The importance of considering energy parameters to describe fatigue

damage is undoubtable, as testified by the generalized approach that has been proposed recently using experimental data of Waspaloy [19]. Anyway, the errors associated to measured strain and stress during test are so high that a notable scatter generally affects calculation of energy parameters. This observation is particularly true in large part of the test carried out in this work, where elastic behaviour is predominant and the loading and unloading curves are practically coincident. Nevertheless, hysteresis area reported in the previous tables can be correlated to the resulting stress range and a clear correlation exists in all the test conditions (Fig. 3a). On the other hand, it is not possible to use the values of hysteresis area as a damage indicator due to its low magnitude. From a practical point of view, the trends of hysteresis area against fatigue life that have an initial value higher than 0.5 mJ/mm^3 have been considered. Hysteresis area is practically constant or show limited variation up to failure (Fig. 3b). Therefore, the use of energy indicator related to hysteresis area to describe damage phenomena has a limited importance for the stress-strain level that is usually present in the working condition of an industrial component.

	Strain Range $\Delta\varepsilon/\Delta\varepsilon_{max}$	*Cycles to failure* N_f/N_{max}	*Normalized Stress Range* $\Delta\sigma/\Delta\sigma_{max}$	*Stress Ratio* $R = \sigma_{min}/\sigma_{max}$	*Hysteresis Area* H [mJ/mm^3]	*Tangent Modulus* E_T [N/mm^2]
TIG-RT-1	0.767	0.0011	0.5352	-0.15	0.169	143012
TIG-RT-2	0.581	0.0203	0.7324	-1.18	0.217	222952
TIG-RT-3	0.795	0.0041	0.9081	-0.66	0.551	216812
TIG-RT-4	0.472	0.0157	0.5677	-0.20	0.042	211581
TIG-RT-5	0.473	0.0179	0.5664	-0.08	0.035	213285
TIG-RT-6	0.571	0.0617	0.6718	-3.94	0.702	217488
TIG-RT-7	0.472	0.0095	0.5389	-0.17	0.404	209687
TIG-RT-8	0.690	0.0084	0.8389	-0.57	0.144	213285
TIG-RT-9	0.795	0.0022	0.8065	-0.46	0.089	143342
TIG-RT-10	0.476	0.0328	0.5462	-0.16	0.162	203959
TIG-RT-11	0.584	0.0146	0.6691	-0.27	0.081	200947
TIG-RT-12	0.584	0.0105	0.6883	-0.34	0.125	205143
TIG-RT-13	0.804	0.0014	0.8598	-0.59	0.235	196114
TIG-RT-14	0.476	0.0308	0.5407	-0.11	0.087	203601

Table 4: TIG Welded Material – Room Temperature: fatigue test results.

	Strain Range $\Delta\varepsilon/\Delta\varepsilon_{max}$	*Cycles to failure* N_f/N_{max}	*Normalized Stress Range* $\Delta\sigma/\Delta\sigma_{max}$	*Stress Ratio* $R = \sigma_{min}/\sigma_{max}$	*Hysteresis Area* H [mJ/mm^3]	*Tangent Modulus* E_T [N/mm^2]
TIG-538-3	0.686	0.0031	0.4097	-0.35	0.112	162957
TIG-538-4	0.660	**0.1699**	0.4905	-0.21	0.032	133696
TIG-538-5	0.675	0.0200	0.6552	-0.34	0.161	147811
TIG-538-6	0.801	0.0027	0.6730	-0.53	0.169	149473
TIG-538-8	0.516	0.0272	0.4562	-0.11	0.029	153746
TIG-538-9	0.660	**0.0804**	0.4764	-0.21	0.031	129936
TIG-538-11	0.794	0.0040	0.5328	-0.09	0.283	137832
TIG-538-12	0.574	0.0049	0.4525	-0.06	0.027	135120
TIG-538-13	0.551	**1.0000**	0.3246	0.16	0.092	131529
TIG-538-14	0.676	0.0160	0.4133	0.02	0.144	124787
TIG-538-16	0.780	0.0009	0.6105	-0.26	0.038	139634
TIG-538-17	0.789	0.0095	0.6203	-0.45	0.040	141017
TIG-538-18	0.684	0.0105	0.4146	0.07	0.046	103570
TIG-538-19	0.589	0.0240	0.5909	-0.18	0.081	131791

Table 5: TIG Welded Material – 538°C: fatigue test results.

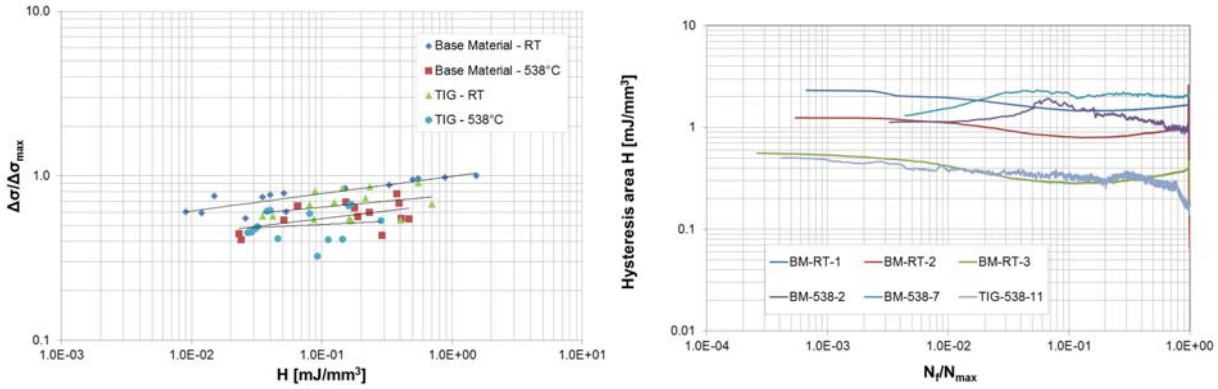

Figure 3: Correlation between resulting stress range and hysteresis area (a) and hysteresis area trend against fatigue life (b).

Fig. 4 reports an example of an hysteresis cycle, while the change of peak stress for two tests carried out at a strain range $\Delta\varepsilon/\Delta\varepsilon_{max} = 0.44$ is showed in Fig. 5. Material plastic behaviour is very limited and the stress range is practically constant for the whole life of the specimen, with the exclusion of the last cycles, when a fatigue crack initiation process is already started. Similar trends are obtained for TIG welded specimen and at high temperature also.

Change of tangent modulus E_T and hysteresis area H is generally considered an important indicator of the progress of the damage process in the material. Crack initiation has the effect to reduce specimen stiffness and a measurable reduction of the tangent modulus is showed. Hysteresis area represents the work associated to plastic deformation in each load cycle [20], which is partially stored in the material as a potential damage and partially dissipated as heating [21]. Therefore, these two parameters have been calculated starting from the whole data cycle and correlated to number of cycles for each specimen. An example of tangent modulus E_T trend is reported in Fig. 6. Observing this last graph, it is possible to show that the decay of tangent modulus is always measurable only at the end of life, when a crack is already present. Consequently, this parameter has a limited interest to follow the damage evolution in the material. Moreover, the trends of hysteresis area H (Fig. 3b) have no practical utility, due to its low values.

From a quantitative point of view, fatigue behaviour of base and TIG welded material is synthetically expressed by the fatigue curves in terms of applied strain range (Fig. 7) or in terms of measured stress range (Fig. 8). In all the conditions, TIG welded material shows a lower fatigue curve than base material. The reduction of fatigue strength can be quantified interpolating the experimental data to calculate Basquin's law and finally the strain range $\Delta\varepsilon_A$ and the stress range $\Delta\sigma_A$ corresponding to a reference life N_{ref} (Tab. 6). A careful analysis of these data reveals that the fatigue strength expressed in terms of strain range $\Delta\varepsilon_A$ is increased when temperature test changes from RT to 538°C. On the contrary, fatigue stress in terms of stress range $\Delta\sigma_A$ is reduced in the same condition.

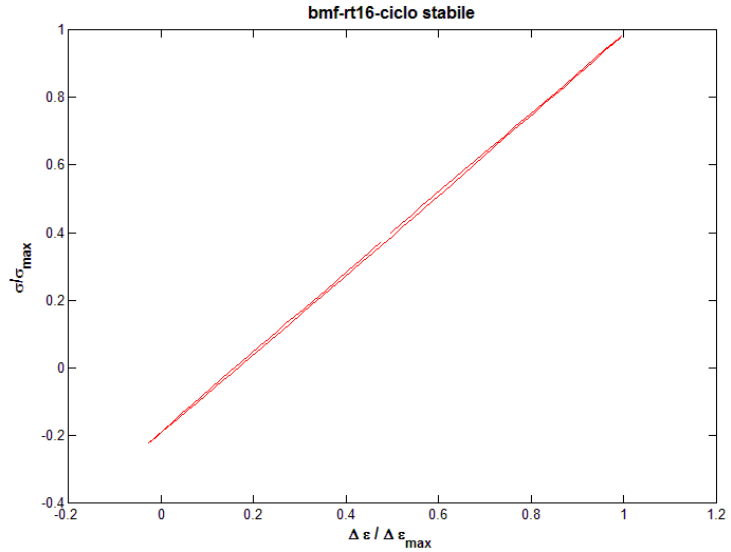

Figure 4: Example of stabilized hysteresis cycle.

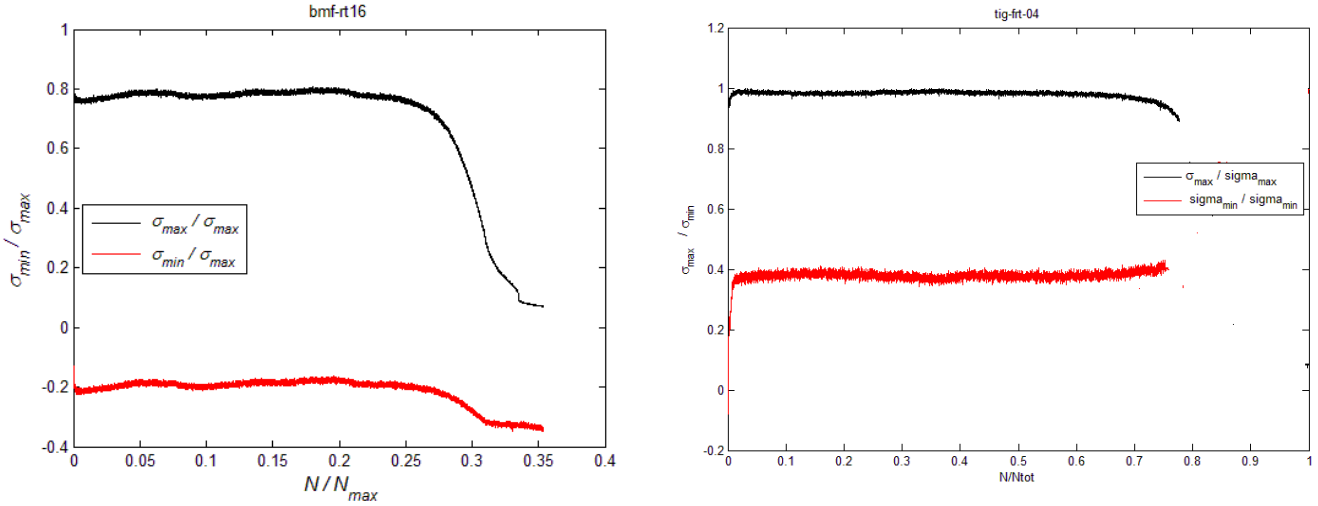

(a) (b)

Figure 5: Peak stress trend of a base (a) and TIG welded specimen (b).

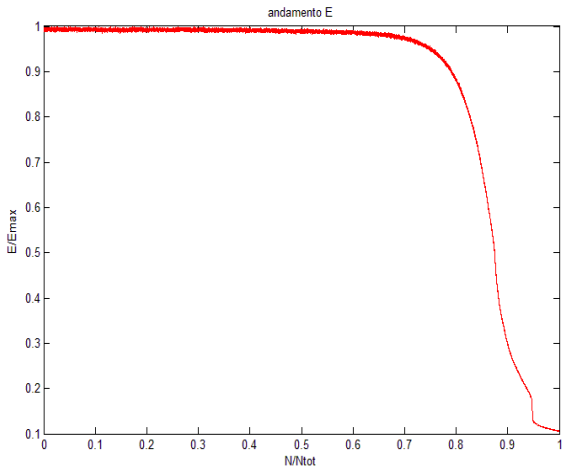

Figure 6: Example of tangent modulus E_T trend

This behaviour is clearly confirmed by the experimental data both for base and TIG welded material. However, not only this observation is not reported in any experimental work existing in literature, but also it is not verified for other experimental data obtained using standard circular specimen. It is very difficult to indicate a clear explanation, but some hypothesis can be formulated. A possibility is to invoke a complex interaction between fatigue and creep damage, which become relevant when applied strain is so low that the load cycle can be considered fully elastic and the test duration is over 24 hours. Another possibility is to consider that the specimens have been obtained by a laminated plate rather than round bars, as usual: the different influence of the residual stress field existing in the laminated plate could shows its detrimental effect only at Room Temperature, while at higher temperature relaxation phenomena could mitigate the effects. However, no quantitative data or qualitative observations are available to support one hypothesis with respect to others and this constitutes an open problem.

Creep test.

Creep strength of base and TIG welded material has been expressed in terms of time to reach a fixed inelastic strain or failure (Tab. 7). Also in this case data reported in Tab. 3 are normalized with respect to the maximum measured life and represents the mean values over 3 specimens. It is interesting to observe that TIG specimens show a lower time to reach a fixed strain or failure but only if the lower stress level is considered. At a stress level of 475 N/mm², creep strength is

increased, with the exception of failure. At this purpose, the failure of TIG specimens happen roughly, without showing the increase of strain rate that usually characterizes the tertiary creep behaviour (Fig. 9).

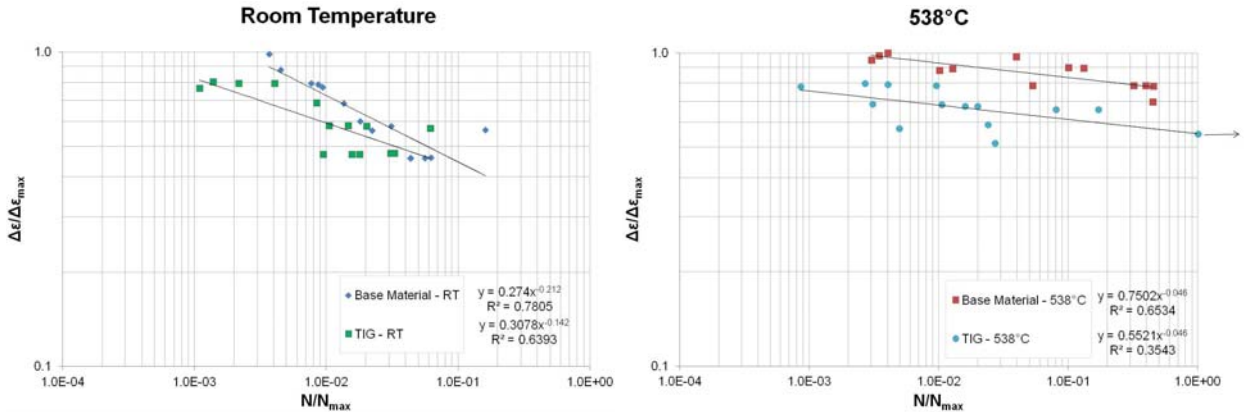

(a) (b)

Figure 7: Comparison of fatigue curves in terms of applied strain range at RT (a) and 538°C (b).

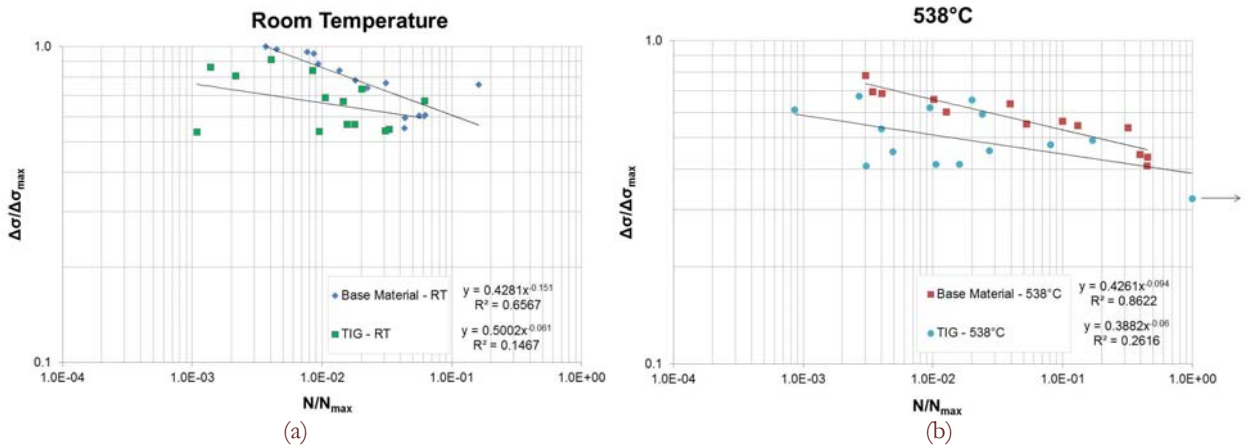

(a) (b)

Figure 8: Comparison of fatigue curves in terms of measured stress range at RT (a) and 538°C (b).

	$\Delta\sigma_A/\Delta\sigma_{max}$			$\Delta\varepsilon_A/\Delta\varepsilon_{max}$ [%]		
	Base Material	*TIG*	*var %*	*Base Material*	*TIG*	*var %*
RT	0.673	0.601	-10.7	0.516	0.433	-8.6
538°C	0.565	0.464	-17.9	0.862	0.581	-26.5

Table 6: Fatigue strength at N_{ref} cycles of base material and TIG.

	time [h/h_{max}]														
σ	ε_c = 0.2%			ε_c = 0.5%			ε_c = 1%			ε_c = 2%			failure		
N/mm²	BM	TIG	var %	BM	TIG	var %	BM	TIG	var %	BM	TIG	var %	BM	TIG	var %
427.5	0.0372	0.0057	-84	0.0976	0.0406	-58	0.1919	0.1431	-25	0.4047	0.3616	-10	1.0000	0.6107	-38
475	0.0006	0.0010	57	0.0023	0.0042	83	0.0167	0.0190	13	0.0336	0.0606	80	0.2743	0.1178	-57

Table 7: Creep behaviour of base material and TIG.

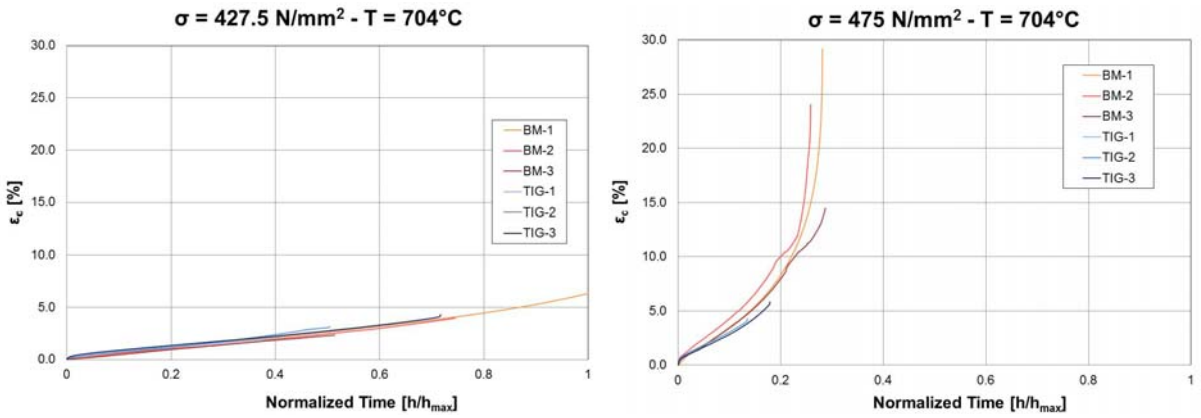

Figure 9: Creep deformation against normalized time at 427.5 MPa (a) and 475 MPa (b).

Conclusion

Base and TIG welded Waspaloy has been mechanically tested and static, low-cycle fatigue and creep behaviour have been evaluated. The comparison of the experimental data between base and TIG welded material allowed calculating the reduction of the material performance for each mechanical property. The low level of the applied strain in a large number of fatigue tests constituted a limitation in order to utilize damage models for fatigue life prediction.

Acknowledgments

This work has been financially supported by Apulia Region in the field of "Program Agreement about Research and Competitivity" approved with Regional Council Deliberation n° 2553 dated 22 December 2009.

References

[1] Taira, S., Fatigue at Elevated Temperatures, American Society for Testing and Materials, Philadelphia, (1973).
[2] Tong, J., Vermeulen, B., The description of cyclic plasticity and viscoplasticity of waspaloy using unified constitutive equations, Int. Journal of Fatigue, 25 (2003) 413-420.
[3] Kneifl, M., Černý, I., Bína, V., Damage of low-alloy high temperature steels loaded by low-cycle fatigue and creep, Int. J. Press. Vessel and Piping ,78 (2001) 921-927.
[4] Yeom, J.T., Williams, S.J., Park, N.K., Low-cycle fatigue life prediction for Waspaloy, Materials at High Temperatures, 19(3) (2002) 153-161.
[5] Garimella, L., Liaw, P., Klarstrom, D., A study of fatigue crack growth behavior of Haynes 242 alloy, JOM, 49 (1997) 67-71.
[6] Cao, M., Gabrielli, F., Pelloux, R., Effect of temperature, loading frequency and heat treatment on fatigue crack growth in a nickel base alloy, Res Mechanica, 17 (1986) 163-177.
[7] Bache, M.R., Evans, W.J., Hardy, M.C., The effects of environment and loading waveform on fatigue crack growth in Inconel 718, Int. Journal of Fatigue, 21 (1999) 69-77.
[8] Goto, M., Yamomoto, T., Kawagoishi, N., Nisitani, H., Growth behaviour of small surface cracks in Inconel 718 superalloy, In: International Conference on Temperature-Fatigue Interaction, Ninth International Spring Meeting, 29 (2002) 237-246.
[9] Tong, J., Dalby, S., Byrne, J., Henderson, M.B., Hardy, M.C., Creep, fatigue and oxidation in crack growth in advanced nickel-base superalloys, Int Journal of Fatigue, 23 (2001) 897-902.

[10] Roy, A.K., Venkatesh, A., Marthandam, V., Ghosh, A., Tensile deformation of a Nickel-base Alloy at elevated temperatures, Journal of Material Engineering and Performance, 17(4) (2008) 607-611.
[11] Li, Z., Gobbi, S.L., Loreau, J.H., Laser welding of Waspaloy sheets for aero-engines, Journal of Mat Processing Tech, 65 (1997) 183-190.
[12] Chamanfar, A., Jahazi, M., Gholipour, J., Wanjara, P., Yue, S., Mechanical property and microstructure of linear friction welded Waspaloy, Metallurgical and Materials Transactions A, 42 (2011) 729-744.
[13] Huang, Z.W., Li, H.Y., Preuss, M., Karadge, M., Bowen, P., Bray, S., Baxter, G., Metall. Mater. Trans. A, 38A (2007) 1608–20.
[14] Adam, P., Welding of High Strength Gas Turbine Alloys, Applied Science Publisher Ltd., London, (1978) 737–68.
[15] Vishwakarma, K.R., Richards, N.L., Chaturvedi, M.C., In: 6th Int. Symp. on Superalloys 718, 625, 706 and Derivatives, E.A. Loria, ed, TMS, Pittsburgh, PA, 2005, 637–47.
[16] Sekhar, N.C., Reed, R.C., Power beam welding of thick section nickel base superalloys, Sci. Technol. Weld. Join., 7 (2002) 77–87.
[17] Ma, T.J., Li, W.Y., Xue, Q.Z., Zhang, Y., Li, J.L., Yang, S.Q., Mater. Sci. Forum, 580–582 (2008) 405–408.
[18] Oja, M., Ravi Chandran, K.S., Tryon, R.G., Orientation imaging microscopy of fatigue crack formation in Waspaloy: crystallographic conditions for crack nucleation, International Journal of Fatigue, 32 (2010) 551–556.
[19] Warren, J., Wei, D.Y., A microscopic stored energy approach to generalize fatigue life stress ratios, Int. Journal of Fatigue, 32 (2010) 1853-1861.
[20] Morrow, J., Cyclic Plastic Strain Energy and Fatigue of Metals, Internal Friction, Damping, and Cyclic Plasticity, ASTM STP 378, Philadelphia PA, (1965) 45-84.
[21] Leis, B.N., An Energy-Based Fatigue and Creep-Fatigue Damage Parameter, J Press Ves Tech Trans ASME, 99 (1977) 524–533.